Voxel-based detection of white matter abnormalities in mild Alzheimer disease

S. Xie, MD; J.X. Xiao, MD; G.L. Gong, PhD; Y.F. Zang, PhD; Y.H. Wang, MD; H.K. Wu, MD; and X.X. Jiang, MD

Abstract—*Objective:* To detect white matter abnormalities in patients with mild Alzheimer disease (AD) by diffusion tensor imaging and to determine their topographic relationship with gray matter atrophy. *Methods:* Thirteen patients with mild AD and 16 normal age-matched volunteers underwent diffusion tensor imaging and three-dimensional spoiled gradient-recalled sequence scanning. Voxel-based morphometry was conducted to detect regions of gray matter atrophy in the AD group relative to the control group. Fractional anisotropy (FA) maps were processed using SPM2 to make voxel-wise comparison of anisotropy in whole brain between the two groups. The relationship between locations of abnormalities in the white and gray matter was examined. *Results:* Significant reductions in anisotropy were found in the white matter of both medial temporal lobes, bilateral temporal stems, bilateral superior longitudinal fasciculi, bilateral internal capsules, and cerebral peduncles, as well as the white matter of left middle temporal gyrus and right superior parietal lobule, the body and genu of the corpus callosum, and the right lateral capsule in patients with AD. Although the decrease in FA was consistent with cortical volumetric reduction in both temporal lobes, the widespread involvement of bilateral superior longitudinal fasciculi was dominant in these white matter findings. *Conclusions:* Voxel-wise comparison of whole-brain anisotropy revealed widely distributed disintegration of white matter in mild Alzheimer disease (AD). The white matter shows a different pattern of degeneration from gray matter and may be an independent factor in the progress of AD.

NEUROLOGY 2006;66:1845–1849

White matter changes have been observed in patients with Alzheimer disease (AD) and are typically described as rarefaction with axonal damage and gliosis attributed to Wallerian degeneration.[1,2] In a previous study, the results suggested that white matter lesions of whole brain and hippocampal atrophy were related in AD.[3] Diffusion tensor imaging (DTI), a noninvasive MRI technique, has been used to detect white matter abnormalities in AD.[4-6] However, the information that based on analysis of regions of interest (ROIs) cannot completely reflect the structural integrity of the fiber tracts. In addition, the relationship between white matter changes and gray matter atrophy cannot be elucidated.

Voxel-based morphometry (VBM) is an automatic way to evaluate differences in brain morphology between patient groups. Different from ROI-based methods, VBM techniques provide a means of investigating volumetric abnormalities automatically over the entire cerebral volume. With this method, some other discrete brain regions such as the posterior cingulate gyrus and bilateral insulae have shown atrophy in the early stage of AD.[7,8] Although VBM has been extensively cross-validated with ROI measurements and functional correlates[9] and has been used in conjunction with measures of neuropsychological function in neurodegenerative disorders,[10] voxel-based comparison of whole-brain white matter anisotropy between AD group and controls is comparatively less studied.[11] The aim of this study was to investigate white matter abnormalities in AD based on voxel-wise comparison with normal controls and to explore their relationship with cortical atrophy detected by VBM.

Methods. *Subjects.* We recruited 13 patients with AD (8 men, 5 women; age range 62 to 82 years; mean age 71.7 years). The diagnosis of probable AD was established according to National Institute of Neurological and Communicative Disorders and Stroke/Alzheimer's Disease and Related Disorders Association criteria. The overall severity of cognitive impairment was rated with the Mini-Mental State Examination (MMSE). Their MMSE score ranged from 19 to 24 with mean of 21.1, and they were classified as mildly impaired. Two patients in the AD group had medication-controlled hypertension, and the remainder had no history of diabetes, coronary heart disease, peripheral vascular disease, or other cardiovascular disease. Sixteen normal aging volunteers (10 men, 6 women; age range 61 to 79 years; mean age 71 years) were recruited from the local community as controls. Controls were defined as individuals who did not have active neurologic or psychological conditions, had no cognitive complains, had no severe systemic disease, and were not taking any psychoactive medicines in doses that would affect their cognition. Their MMSE scores were all above 27. They were matched with patients for education and age. Informed consent for participation was obtained from every subject, and the Ethics Committee at Peking University approved all the protocols used in this study.

MR data acquisition. All MRI was performed on a 1.5 T MR scanner (GE Signa 1.5 T Twinspeed, Milwaukee, WI). Conventional axial T2-weighted images were obtained previously to rule

From the Departments of Radiology (S.X., J.X.X., H.K.W., X.X.J.) and Neurology (Y.H.W.), Peking University First Hospital, and National Laboratory of Pattern Recognition (G.L.G., Y.F.Z.), Institute of Automation, Chinese Academy of Sciences, Beijing, China.

Disclosure: The authors report no conflicts of interest.

Received November 28, 2005. Accepted in final form March 10, 2006.

Address correspondence and reprint requests to Dr. S. Xie, Radiology Department, Peking University First Hospital, 8 Xishiku St, Xicheng District, Beijing, 100034, China; e-mail: ouyangxu2004@vip.sina.com

Table 1 *Regions of significantly reduced gray matter volume in the brains of patients with mild Alzheimer disease (n = 13) vs age-matched control subjects (n = 16)*

Brian region	Side	No. of voxels	*p* value (corrected)	Coordinates *X*, *Y*, *Z*	Peak Z score
Amygdala, hippocampus, parahippocampal gyrus	Right	423	<0.001	20, −6, −24	5.17
Amygdala, hippocampus, parahippocampal gyrus	Left	182	0.002	−18, −8, −22	4.33
Superior temporal gyrus, middle temporal gyrus, inferior temporal gyrus	Right	1,222	<0.001	58, −34, −4	5.21
Superior temporal gyrus	Left	124	0.012	−52, −2, −14	4.39
Middle temporal gyrus	Left	164	0.003	−58, −26, −10	4.67
Insula	Right	516	<0.001	38, 0, 10	5.45
Prefrontal lobe	Left	188	0.001	−42, 28, −12	4.87
Anterior cingulate gyrus, gyrus rectus, caudate nuclei, subcallosal region, basal forebrain	Bilateral	1,298	<0.001	12, 14, −2	5.42
Medial thalamus	Bilateral	729	<0.001	8, −16, 6	5.03

out cerebral infarction or other lesions. Diffusion tensor imaging was acquired with a single-shot echo planar imaging (EPI) sequence in alignment with the anterior–posterior commissure plane. The diffusion-sensitizing gradients were applied along 13 noncollinear directions with b value of 1,000 s/mm^2, together with an acquisition without diffusion weighting ($b = 0$). Thirty contiguous axial slices were acquired with 4-mm thickness and no gap. The acquisition parameters were as follows: repetition time (TR) = 10,000 milliseconds; echo time (TE) = 80 milliseconds; matrix = 128 × 128; field of view (FOV) = 24 × 24 cm; no. of excitations (NEX) = 2. After that, high-resolution three-dimensional spoiled gradient-recalled (SPGR) images (TR = 11.3 milliseconds, TE = 4.2 milliseconds, inversion time = 400 milliseconds, FOV = 24 × 24 mm, matrix = 256 × 192, slice thickness = 1.6 mm, NEX = 3) covering the whole brain were also obtained.

Data processing. For gray matter analysis, three-dimensional SPGR images were processed with the method of standard VBM. With use of SPM2 (Wellcome Department of Cognitive Neurology, London, UK), first an affine and nonlinear spatial normalization of the raw MRI sets was performed, and then they were segmented to extract the gray matter tissue. The extracted gray matter set was then smoothed with 8-mm full width at half-maximum Gaussian filter to reduce confounding by individual variation in gyral anatomy and to increase the signal-to-noise ratio. The data (without normalization for the total amount of gray matter) of the two groups of subjects were then compared using the Student t test. The threshold used for selection of voxels was 40% of the grand mean value. In addition, the proportional scaling routine was used, which normalized the gray matter sets across subjects to the overall grand mean. This ancillary analysis was meant to assess the relative distribution of gray matter atrophy in AD compared with controls. Implicit masking was used to ignore zeros, and global calculation was based on the mean voxel value.[7] We set our statistical threshold for the atrophy studies relative to control subjects at a value of $p < 0.001$.

The threshold used for selection of clusters was 50 contiguous voxels. The statistical maps are produced in standardized brain space showing the location of voxel clusters where significant differences in mean gray matter volumes were detected.

Diffusion tensor images were first processed with the GE workstation to generate fractional anisotropy (FA) maps. To allow voxel-by-voxel statistical comparison to be made, the $b = 0$ images of all control subjects and patients were normalized to the standard EPI template of SPM2 using an affine and nonlinear spatial normalization algorithm. Then the FA maps were normalized by applying the normalization parameters determined from the normalization of the $b = 0$ images. Voxel-by-voxel between-group comparisons of FA were investigated at a statistical threshold of $T > 3.42$ ($p < 0.001$, uncorrected for multiple comparisons) using the Student t test. The threshold used for selection of clusters was 50 contiguous voxels. The significant voxels were superimposed on the mean FA map of the AD group to generate a pseudo-color map. Because misregistration of FA maps can lead to false-positive results, we presumed that only those voxels located in the center of the fiber tracts could be reliably interpreted. To minimize false-positive results, a mask was used to exclude those clusters that were superimposed on the voxels with FA being no more than 0.3. Additionally, the voxels in the ventricles and thalami were masked manually. By using the mask, voxel clusters that were around the ventricles and at the edge of fiber tracts were then excluded.

Results. There was no statistical difference in age between the two groups (71.7 ± 6.7 years for patients with AD, 71 ± 6.1 years for controls).

The statistical parametric map investigating the regional location of reductions in gray matter volume in the AD group relative to controls showed several voxel clusters distributed bilaterally over the hippocampi and amygdalae, parahippocampal gyri and medial thalami, caudate nuclei, rectus gyri, anterior cingulate gyri, basal forebrain, superior and middle temporal gyri, as well as in the left prefrontal lobe, right insula, and right inferior temporal gyrus. They were all significant at the uncorrected $p < 0.001$ cluster level. Details about their peak significance and cluster size are provided in table 1. After correction for multiple comparisons, these clusters remained significant at the level of $p < 0.05$.

Significant reductions in anisotropy of the AD group relative to controls were found in several white matter regions, including bilateral medial temporal lobes, bilateral temporal stems, bilateral superior longitudinal fasciculi, bilateral internal capsules, and cerebral peduncles, as well as the left middle temporal gyrus, left body of corpus callosum, genu of corpus callosum, right lateral capsule, and right superior parietal lobule (table 2).

The figure displays the foci of reduced gray matter volume and FA in patients with AD relative to control subjects. As we expected, the foci of lower FA in patients with AD were close to those of cortical volume reduction in some sites, including the bilateral medial temporal lobes, left middle temporal gyrus, and right insula, but there were remarkable exceptions. The white matter abnormalities within the right superior parietal lobule, bilateral superior longitudinal fasciculi, and cerebral peduncles were structurally distant from the atrophic cortices revealed in this study.

Table 2 *Regions of significantly reduced fractional anisotropy in brains of patients with mild Alzheimer disease (n = 13) vs age-matched control subjects (n = 16)*

Location of white matter	Side	No. of voxels	*p* value (corrected)	Coordinates *X*, *Y*, *Z*	Peak Z score
Medial temporal lobe, temporal stem	Right	107	<0.001	34, −6, −28	4.72
Medial temporal lobe, temporal stem	Left	56	<0.001	−30, −6, −14	4.01
Middle temporal gyrus, posterior	Left	65	<0.001	−48, −22, −16	4.18
Lateral capsule	Right	66	<0.001	24, 8, −14	4.72
Superior longitudinal fasciculus, posterior	Left	318	<0.001	−32, −62, 6	5.93
Superior longitudinal fasciculus, anterior	Left	167	<0.001	−26, −30, 4	5.19
Superior longitudinal fasciculus, posterior	Right	195	<0.001	28, −62, 16	5.10
Superior parietal lobule	Right	172	<0.001	18, −54, 44	5.27
Corpus callosum, anterior forceps	Right	71	<0.001	16, 36, −4	5.02
Corpus callosum, anterior forceps	Left	112	<0.001	−20, 34, −6	5.60
Corpus callosum, body	Left	131	<0.001	−18, 6, 34	4.68
Internal capsule, cerebral peduncle	Right	125	<0.001	14, −20, −16	4.59
Internal capsule, cerebral peduncle	Left	116	<0.001	−20, −14, 6	4.92

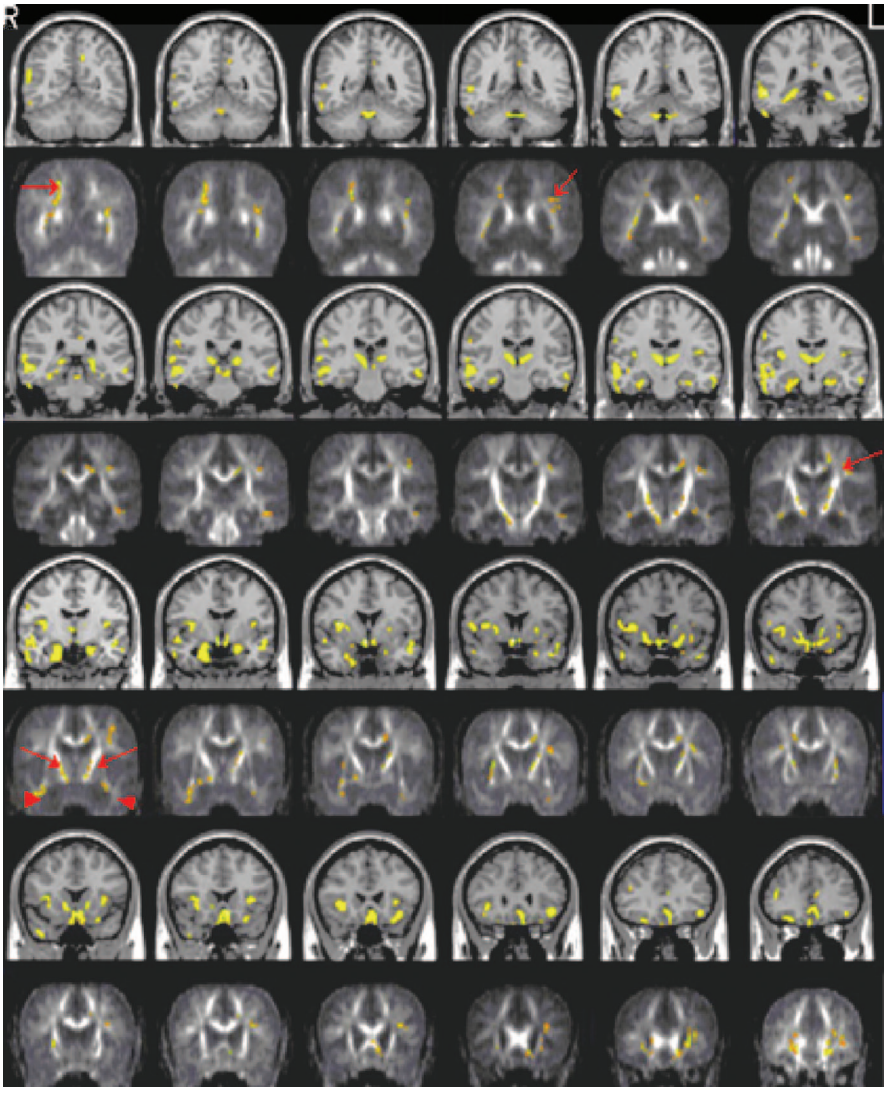

Figure. The foci of reduced gray matter volume (upper row) and fractional anisotropy (FA) (lower row) in patients with Alzheimer disease (AD) relative to control subjects are illustrated in corresponding coronal slices from Y = −56 to Y = 36. The significant voxels of reduced gray matter volume are superimposed on the T1 template provided by SPM2, whereas the clusters of decreased FA in patients with AD are shown on the mean FA map of the AD group. Regions of lower FA in patients with AD consistent with adjacent cortical volume reduction are indicated with arrowheads (medial temporal lobes). The arrows indicate those regions with decreased FA independent of gray matter volume reduction (right superior parietal lobule, bilateral superior longitudinal fasciculi, and bilateral internal capsules).

Discussion. This study provides a detailed depiction of the structural changes in early AD. Multiple areas of white matter change, in addition to gray matter atrophy, were detected in whole brain from patients with AD relative to age-matched control subjects. Consistent with previous imaging studies,[12-14] our study showed significant volumetric reduction of the hippocampi and amygdalae in patients with AD. In addition, our study revealed involvement of a number of other cortical areas including bilateral insulae and bilateral medial thalami.

Although AD is generally considered to affect primarily gray matter, histopathologic studies show evidence of white matter change, including axonal and oligodendrocyte loss coincident with a reactive astrocytosis. As loss of brain tissue organization can cause a decrease in anisotropy, DTI can provide a meaningful measure of fiber tract organization.[15,16] Changes in the structural integrity can be measured with this technique, and previous studies have demonstrated its usefulness in AD and normal control subjects.[17] By voxel-based analysis of FA in whole brain, we can inspect the pattern of white matter changes in AD and subsequently examine their relationship with cortical atrophy. In our study, several clusters including the white matter of bilateral medial temporal lobes, bilateral superior longitudinal fasciculi, and bilateral internal capsules were defined as significantly different in brains of patients with AD. As the patients with AD in this study had no or only mild changes on T2-weighted images, the white matter changes seen in our study cannot be explained by periventricular hyperintensity.

Some findings in our study support the idea of Wallerian-type degeneration of white matter in mild AD. In particular, the distribution of decreased FA is closely related to the location of cortical atrophy in some regions, for example, bilateral medial temporal lobes. It is perhaps of note that these lobes contain major efferent connections of both amygdalae and hippocampi.

Though there were some abnormal white matter regions adjacent to regions of cortical atrophy, the significant voxels were primarily gathered in the largest association fibers, which were bilateral superior longitudinal fasciculi. Previous DTI research has suggested the superior longitudinal fasciculi can be divided into four subcomponents: SLF I, SLF II, SLF III, and arcuate fasciculus vertical.[18] Our data suggest that the SLF II subcomponent was primarily affected in the AD group. The SLF II is a bidirectional pathway in humans between the prefrontal cortex and the parietal lobe and is involved in perception and focusing of attention in different parts of space. Damage to SLF II could result in disorders of spatial working memory by interrupting relationships with prefrontal area.[4,6,19] In a previous work, bilateral superior longitudinal fasciculi of parieto-occipital regions were reported to be abnormal in AD.[4] However, our results allowed visualization of the abnormalities in their entirety: The left superior longitudinal fasciculi was affected more than previously believed, with changes extending from the posterior to the anterior brain. Apart from SLF II, the significant voxels that were distributed in the white matter of right superior parietal lobule were likely to be part of the right SLF I. The arcuate fasciculus vertical, which runs contiguously with the fibers of SLF II, was also found to be involved bilaterally. The former tract is thought to contribute to the regulation of higher aspects of motor behavior, and the latter provides a means by which the prefrontal cortex can receive and modulate audiospatial information. Our findings indicated that the widespread disintegration of the superior longitudinal fasciculi might give rise to the various neuropsychological deficits in AD.

Although the previous study failed to detect any abnormality within the corticospinal tract,[4] our data showed significant decline in anisotropy within bilateral internal capsules and bilateral cerebral peduncles in the brains of patients with AD that may indicate corticospinal tract involvement. Because of the crowding of corticothalamic and thalamocortical fibers within the internal capsule, it may be more than the corticospinal tract that is affected. Though it is a widely held view that disability in motor function is a late symptom of AD, the presence of motor dysfunction in moderate and even very mild AD has been reported,[20,21] and it is possible that the abnormalities found within the internal capsule are responsible for this motor impairment. However, this finding was unexpected and raises the question of how closely changes in anisotropy correlate with clinical symptoms.

Independent of masking, the anterior forceps and body of the corpus callosum exhibited significant difference in FA between the AD and control groups in our study. There is current debate about the change of regional anisotropy of corpus callosum in AD.[4,6,11] The inclusion of more severe patients with AD in some studies may introduce the emergence of significant AD effects on the corpus callosum. As indicated previously, the severity of age-related myelin breakdown is regionally heterogeneous, with the genu being more extensively involved than the splenium.[22] It was suggested that differences in myelin properties make later-myelinating regions more susceptible to this process. In AD, this process is globally exacerbated, consistent with an extracellular deleterious process such as amyloid β-peptide toxicity.[23]

Although extensive abnormalities of white matter have been identified in this study, we failed to show any changes within the cingulum bundles, which have been reported to be abnormal in some studies.[4,6] It is possible that the cingulum bundles remained relatively intact in our mild AD group. In contrast to the cingulum bundles, some regions within the limbic system, for example, the anterior cingulate gyrus and basal forebrain, were found to be atrophic. The basal forebrain contains the nucleus basalis of Meynert, the origin of cholinergic input to the cerebral

cortex, and is critical in cortical arousal and motivation. Its dysfunction has been implicated in the genesis of memory deficits in AD.[24]

Overall, our findings indicate a reduction in anisotropy primarily within the brain's association regions. Recent studies have confirmed that myelination continues until middle age within the brain's association regions,[25] followed by a subsequent breakdown in the myelin sheaths. This demyelination is especially striking in late-myelinating fiber systems.[26] Age-related myelin breakdown has been visualized on electron microscopy and consists primarily of splits in the lamellae of the myelin sheaths or ballooned sheaths in the absence of changes in or loss of neurons or synapses.[27] In AD, similar myelin abnormalities have been described in the absence of axonal damage.[28] These may be the DTI-detectable white matter changes we have discussed here. Once myelin's function in saltatory conduction is compromised, transmission velocity is reduced and the refractory period of the axon is markedly increased.[29] Myelin degeneration may be a major factor in the decline of higher cognitive functions, which is associated with aging itself and can be exacerbated by the process of AD.[30]

Although voxel-based analysis can automatically reveal abnormalities of entire brain, it is not without limitations and problems.[31] First, different processing parameters will result in different results. Second, the templates provided by SPM are from normal adults and are potentially less suitable for older people. Third, misregistration will cause some problems, which is more severe in voxel-based comparison of FA. Well-organized fiber tracts have greater FA than adjacent randomly arranged white matter, and FA is decreased in the peripheral parts of fiber tracts due to partial volume effect, producing false-positive results. In an attempt to improve the specificity of lesion detection, only patients with mild AD were included in this study, and masking around the ventricles and fiber tracts was used to minimize the effect of misregistration.

Acknowledgment

The authors thank Dr Alex Headley for translating and proofreading this manuscript.

References

1. Scheltens P, Barkhof F, Leys D, et al. Histopathologic correlates of white matter changes on MRI in Alzheimer's disease and normal aging. Neurology 1995;45:883–888.
2. Smith CD, Snowdon DA, Wang H, et al. White matter volumes and periventricular white matter hyperintensities in aging and dementia. Neurology 2000;54:838–842.
3. de Leeuw FE, Barkhof F, Scheltens P. White matter lesions and hippocampal atrophy in Alzheimer's disease. Neurology 2004;62:310–312.
4. Rose SE, Chen F, Chalk JB, et al. Loss of connectivity in Alzheimer's disease: an evaluation of white matter tract integrity with colour coded MR diffusion tensor imaging. J Neurol Neurosurg Psychiatry 2000;69:528–530.
5. Bozzali M, Falini A, Franceschi M, et al. White matter damage in Alzheimer's disease assessed in vivo using diffusion tensor magnetic resonance imaging. J Neurol Neurosurg Psychiatry 2002;72:742–746.
6. Satoshi T, Hisashi Y, Junko T, Masako K, Takashi I, Hideo T. Selective reduction of diffusion anisotropy in white matter of Alzheimer disease brains measured by 3.0 Tesla magnetic resonance imaging. Neurosci Lett 2002;332:45–48.
7. Baron JC, Chetelat G, Desgranges B, et al. In vivo mapping of gray matter loss with voxel-based morphometry in mild Alzheimer's disease. Neuroimage 2001;14:298–309.
8. Chetelat G, Desgranges B, De La Sayette V, et al. Mapping gray matter loss with voxel-based morphometry in mild cognitive impairment. Neuroreport 2002;13:1939–1943.
9. Good CD, Scahill RI, Fox NC, et al. Automatic differentiation of anatomical patterns in the human brain: validation with studies of degenerative dementias. Neuroimage 2002;17:29–46.
10. Gee J, Lijun D, Zhiyong X, et al. Alzheimer's disease and frontotemporal dementia exhibit distinct atrophy–behavior correlates: a computer-assisted imaging study. Acad Radiol 2003;10:1392–1401.
11. Head D, Buckner RL, Shimony JS, et al. Differential vulnerability of anterior white matter in nondemented aging with minimal acceleration in dementia of the Alzheimer type: evidence from diffusion tensor imaging. Cereb Cortex 2004;14:410–423.
12. Hampel H, Teipel SJ, Bayer W, et al. Age transformation of combined hippocampus and amygdala volume improves diagnostic accuracy in Alzheimer's disease. J Neurol Sci 2002;194:15–19.
13. Frisoni GB, Laakso MP, Beltramello A, et al. Hippocampal and entorhinal cortex atrophy in frontotemporal dementia and Alzheimer's disease. Neurology 1999;52:91–100.
14. Lehericy S, Baulac M, Chiras J, et al. Amygdala-hippocampal MR volume measurements in the early stage of Alzheimer disease. AJNR Am J Neuroradiol 1994;15:929–937.
15. Pierpaoli C, Jezzard P, Basser PJ, et al. Diffusion tensor MR imaging of the human brain. Radiology 1996;201:637–648.
16. Beaulieu C. The basis of anisotropic water diffusion in the nervous system—a technical review. NMR Biomed 2002;15:435–455.
17. Bartzokis G, Cummings J, Sultzer D, Henderson VW, Nuechterlein KH, Mintz J. White matter structural integrity in aging and Alzheimer's disease: a magnetic resonance imaging study. Arch Neurol 2003;60:393–398.
18. Nikos M, Kennedy DN, McInerney S, et al. Segmentation of subcomponents within the superior longitudinal fascicle in humans: a quantitative, in vivo, DT-MRI study. Cereb Cortex 2005;15:854–869.
19. Preuss TM, Goldman-Rakic PS. Connections of the ventral granular frontal cortex of macaques with perisylvian premotor and somatosensory areas: anatomical evidence for somatic representation in primate frontal association cortex. J Comp Neurol 1989;282:293–316.
20. Goldman WP, Baty JD, Buckles VD, Sahrmann S, Morris JC. Motor dysfunction in mildly demented AD individuals without extrapyramidal signs. Neurology 1999;53:956–962.
21. Pettersson AF, Olsson E, Wahlund LO. Motor function in subjects with mild cognitive impairment and early Alzheimer's disease. Dement Geriatr Cogn Disord 2005;19:299–304.
22. Bartzokis G, Sultzer D, Po HL, Nuechterlein KH, Mintz J, Cummings JL. Heterogeneous age-related breakdown of white matter structural integrity: implications for cortical "disconnection" in aging and Alzheimer's disease. Neurobiol Aging 2004;25:843–851.
23. Wisniewski HM, Bancher C, Barcikowska M, Wen GY, Currie J. Spectrum of morphological appearance of amyloid deposits in Alzheimer's disease. Acta Neuropathol 1989;78:337–347.
24. Shinotoh H, Namba H, Fukushi K, et al. Progressive loss of cortical acetylcholinesterase activity in association with cognitive decline in Alzheimer's disease: a positron emission tomography study. Ann Neurol 2000;48:194–200.
25. Ge Y, Grossman RI, Babb JS, Rabin ML, Mannon LJ, Kolson DL. Age-related total gray matter and white matter changes in normal adult brain. Part I: volumetric MR imaging analysis. AJNR Am J Neuroradiol 2002;23:1327–1333.
26. Hildebrand C, Remahl S, Persson H, Bjartmar C. Myelinated nerve fibres in the CNS. Prog Neurobiol 1993;40:319–384.
27. Peters A, Moss MB, Sethares C. Effects of aging on myelinated nerve fibers in monkey primary visual cortex. J Comp Neurol 2000;419:364–376.
28. Umahara T, Tsuchiya K, Ikeda K, Kanaya K, Iwamoto T, Takasaki M, et al. Demonstration and distribution of tau-positive glial coiled body-like structures in white matter and white matter threads in early onset Alzheimer's disease. Neuropathology 2002;22:9–12.
29. Felts PA, Baker TA, Smith KJ. Conduction in segmentally demyelinated mammalian central axons. J Neurosci 1997;17:7267–7277.
30. Bartzokis G. Age-related myelin breakdown: a developmental model of cognitive decline and Alzheimer's disease. Neurobiol Aging 2004;25:5–18.
31. Ashburner J, Friston KJ. Voxel-based morphometry—the methods. Neuroimage 2000;11:805–821.